

Phase transition in the collective migration of tissue cells: experiment and model

B. Szabó,¹ G. J. Szöllősi,¹ B. Gönci,¹ Zs. Jurányi,¹ D. Selmeczi,¹ and Tamás Vicsek^{1,2}

¹ Department of Biological Physics, Eötvös University, Pázmány P. stny. 1A, H-1117 Budapest, Hungary

² Biological Physics Research Group of HAS, Pázmány P. stny. 1A, H-1117 Budapest, Hungary

(October 11, 2018)

We have recorded the swarming-like collective migration of a large number of keratocytes (tissue cells obtained from the scales of goldfish) using long-term videomicroscopy. By increasing the overall density of the migrating cells, we have been able to demonstrate experimentally a kinetic phase transition from a disordered into an ordered state. Near the critical density a complex picture emerges with interacting clusters of cells moving in groups. Motivated by these experiments we have constructed a flocking model that exhibits a continuous transition to the ordered phase, while assuming only short-range interactions and no explicit information about the knowledge of the directions of motion of neighbors. Placing cells in microfabricated arenas we found spectacular whirling behavior which we could also reproduce in simulations.

PACS numbers: 87.17.Aa, 87.17.Jj, 87.64.Rr

I. INTRODUCTION

The collective motion of organisms is a spectacular phenomenon sometimes involving huge schools of fish, thousands of birds exhibiting complex aerial displays [1], herds of quadrupeds and even bacteria producing fractal colonies [2] or amoeba assembling into rotating aggregates [3]. Recently, sperm cells were also demonstrated to form self-organized vortices [4]. In addition to being a common mechanism by which organisms self-organize, a deeper understanding of the simultaneous adjustment of the velocities of many moving objects has important potential applications ranging from the swarming of distributed robots exploring new territories [5] to the healing of wounds related to the coherent migration of epithelial cells [6].

Although widely observed in nature, collective motion is less accessible for experimental investigations under laboratory conditions. Becco *et al.* [7] have presented interesting but only qualitative results. A well controlled series of experiments aimed at characterizing the nature of the transition from a disordered to an ordered phase in velocity space is so far lacking, even though such experiments would be useful both in providing a quantitative reference for further experimental studies and in prompting more realistic models for group behavior. While laboratory observations have been scarce, a number of models based on self-propelled particles have been developed recently (see, e.g., Refs. [8, 9, 10, 11, 12, 13, 14]) to describe collective motion. In broad terms these models fall into two categories, those which describe the onset of collective motion as a transition to an ordered state in a large noisy system with simple interactions between the particles [8, 9, 10], and those which employ more complicated – consequently more realistic – interactions and focus on the emergent collective dynamics of groups of finite size [11, 12, 13, 14]. A model, however, that combines simple short-ranged interactions, detailed realistic dynamics and a well defined kinetic transition in a large noisy system has not been described so far.

In this paper we present experimental results concerning the collective migration of a large number of tissue cells (kerato-

cytes) using long-term videomicroscopy. As the overall density of the migrating cells is increased, we observe a kinetic phase transition from a disordered (low density) state into an ordered (high density) state, in which most of the cells move in a direction approximately agreeing with their average direction of motion. Just below the transition a complex picture emerges with interacting groups of cells moving in random directions. Motivated by these experimental results we develop a flocking model, which, in contrast to previous models, considers a minimal realistic interaction that assumes no explicit averaging of the directions of motion, while also exhibiting a transition to the ordered phase. Numerical studies indicate that this transition is continuous and belongs to the same universality class as the model of Vicsek *et al.* [8]. These results compel us to imply that the experimental transition described is continuous as well.

II. EXPERIMENTAL SETUP AND RESULTS

Our experimental setup, consisting of a home developed fully computer-controlled time-lapse microscope [15] and a custom made room temperature CO₂ mini-incubator allowed us to carry out long-term videomicroscopy of keratocytes together with a quantitative analysis of their motion. We collected 2–4 fish scales from living goldfish (*Carassius auratus*) with tweezers, and placed them external side up in a 35-mm circular Petri dish similarly to Ref. [16]. Scales were kept in the incubator overnight to allow epidermal keratocyte cells to migrate out from the scales. Before time-lapse microscopy scales were removed, and the cells remaining in the Petri dish were treated with phosphate saline buffer and/or trypsin to obtain cultures of varying density (both compounds reversibly weaken cell-cell and cell-substrate connections, allowing the removal of a controllable percentage of the cells). During the subsequent typically 24-h long time-lapse microscopy experiments we monitored the motion of live keratocyte cells (taking pictures in several fields of view at frequency of 1 shot per minute) in cultures of varying density ranging from sparse ones with very low cell densities to confluent ones with nearly complete coverage. We observed a relatively sharp transition

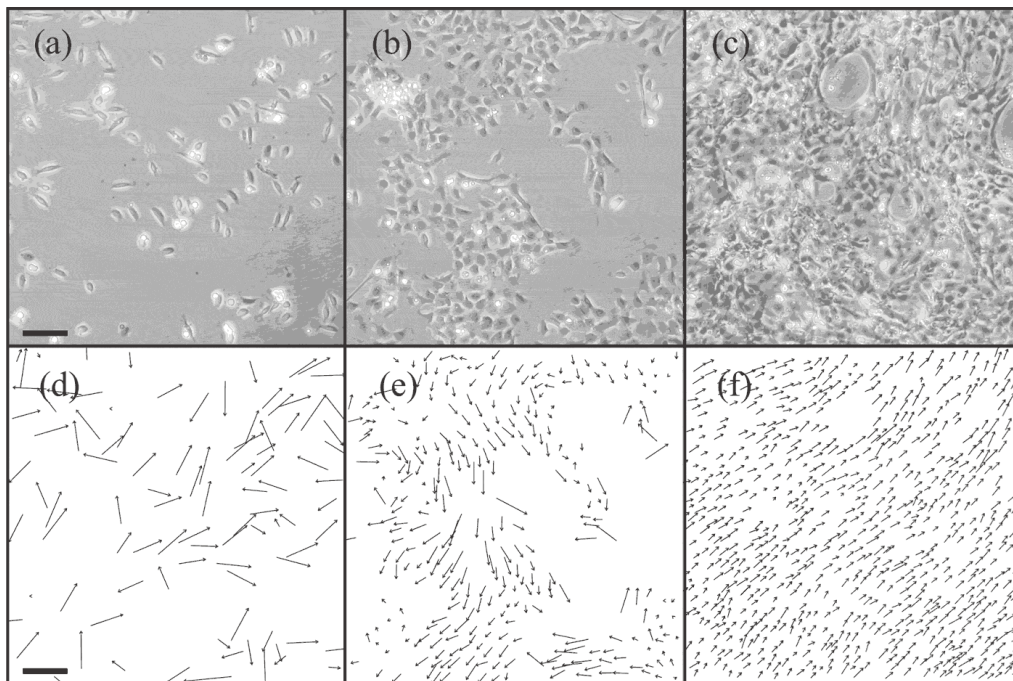


FIG. 1: Phase contrast images showing the typical behavior of cells for three different densities. (a): 1.8, (b): 5.3, (c): 14.7 cells/100x100 μm^2 . We observed that as cell density increases cell motility undergoes collective ordering. The speed of single cells is higher than that of cells moving in coherent groups. Scale bar: 200 μm . (d)-(f): Velocity of cells. Scale bar: 50 $\mu\text{m}/\text{min}$. Online supplemental material [17] contains corresponding videos.

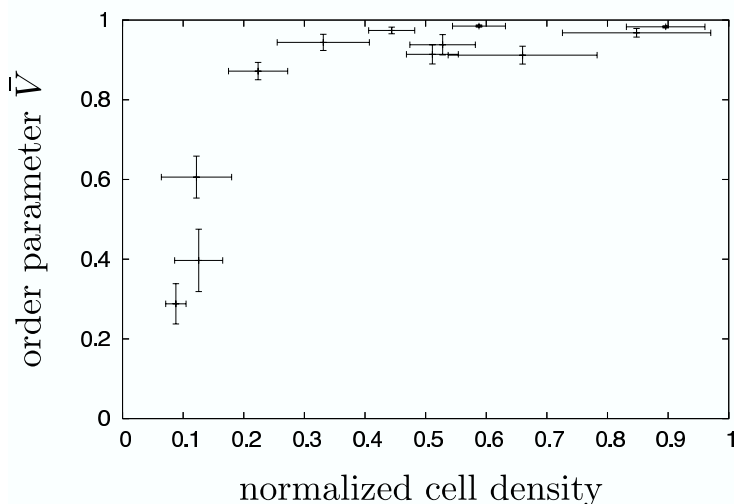


FIG. 2: Order parameter \bar{V} is shown as a function of normalized cell density. Cell density was normalized with the maximal observed density of 2.5×10^{-3} cells/ μm^2 and error bars indicate the standard error of the density and order parameter.

from random motility to an ordered collective migration of dense islands of cells as the density was increased. Fig. 1 shows the typical behavior of cells for three different densities. The technical details of the experiment are described in the online supplemental material [17].

In order to quantify the level of coherence of the migration pattern of cells –the individual motion of which are usually

described as a persistent random walk [18]– we calculated the velocity of 20-30 cells in each experiment from their displacement between frames. This process yielded the $\mathbf{v}_i(t_k)$ velocity vectors of cells, where i is the index of the cell, $t_k = k\Delta t$ is the time elapsed from the start of the cell’s trajectory and Δt denotes the time difference between frames. We define as the measure of coherence of motion an order parameter equal to the time average of the sum of the normalized velocities divided by the number of cells measured. Thus, the order parameter is

$$\bar{V} = \left\langle \frac{1}{N} \left| \sum_{i=1}^N \frac{\mathbf{v}_i(t_k)}{|\mathbf{v}_i(t_k)|} \right| \right\rangle_{t_k}, \quad (1)$$

where N is the number of evaluated cells. Fig. 2 displays the order parameter as a function of cell density. Our measurements were carried out after the cells had had sufficient time to migrate out of the scales and achieve a quasi-stationary migration. \bar{V} was calculated by averaging over the observation time and its standard error was calculated by dividing the standard deviation by $\sqrt{M-1}$, where M is the number of analyzed snapshots. We attempted to survey the extent of finite size effects, by calculating the order parameter and its error, while considering only half the number of available cells. We found no significant deviation. Cell density was measured locally, i.e. in the field of view, every 30 minutes. Both its mean value and the standard error of the mean is presented in Fig. 2. A sharp increase can be observed around 5×10^{-4} cells/ μm^2 .

We conclude that a kinetic phase transition takes place from a disordered into an ordered state as cell density exceeds a

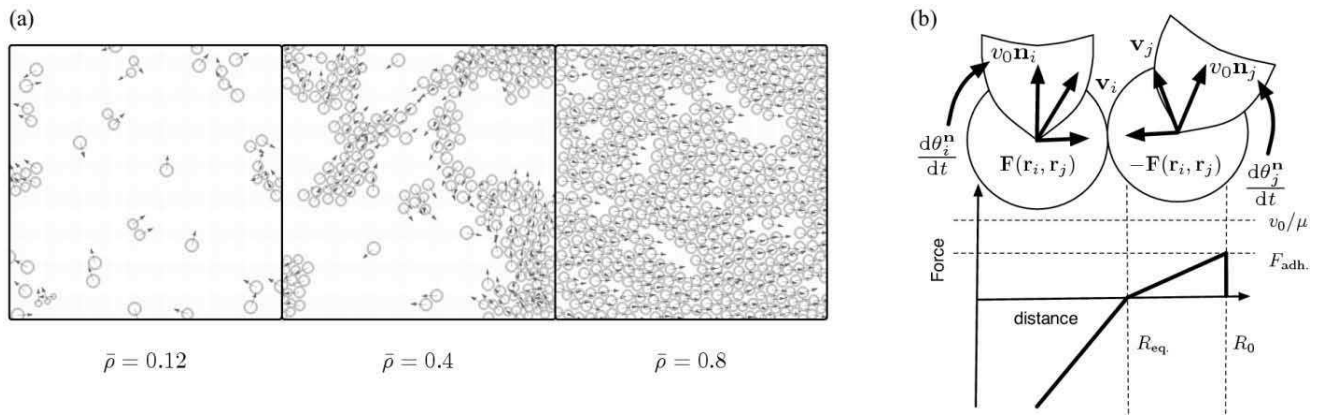


FIG. 3: Computer simulations were performed of the system described in the text for different densities. These simulations showed a transition to the ordered phase similar to that seen in experiments. (a) Typical behavior of cells is shown for three different values of the normalized number density $\bar{\rho} = \rho/\rho_{\max}$, with $\rho_{\max} \approx 2$, which is approximately the density where gaps disappear, and the cells reach tight packing in simulations. (b) As cells moving in different directions come into contact adhesive inter-cellular forces act to align \mathbf{n}_i and \mathbf{n}_j , resulting in an effective averaging of self-driving directions. For videos of simulation runs see the online supplemental material [17].

relatively well-defined critical value. Our experiments suggest that short-range attractive–repulsive intercellular forces alone are sufficient to organize motile keratocyte cells into coherent groups.

III. MODEL DESCRIPTION AND RESULTS

To interpret the above phase transition-like ordering phenomenon we constructed a model that takes into account the specific features of the experimental system and is able to reproduce experiential behavior. In our model individual model cells (self-propelled particles) move forward in a well defined direction with constant speeds. The noisy nature of the processes which generate cell locomotion is taken into account by considering the direction of self-propulsion of model cells to be noisy. Intercellular forces through which model cells interact are considered to be short-ranged, as between keratocytes they are the result of direct physical contact. Further, regarding interactions between keratocyte cells, it is obvious that explicit averaging of the directions of motion employed in previous models is not realistic. Tissue cells forming coherently migrating groups are unable to explicitly adjust their direction of motion to the average velocity of their neighbors, collective motion must emerge solely as a result of direct cell to cell interactions (forces). To model the emergence of collective motion without such explicit averaging, we consider self-propelled particles (model cells) that attempt to adjust their direction of motion toward the direction of the net-force acting on them.

The 2-dimensional motion of model cell $i \in \{1, N\}$ with position $\mathbf{r}_i(t)$ is described by the overdamped dynamics:

$$\frac{d\mathbf{r}_i(t)}{dt} = v_0 \mathbf{n}_i(t) + \mu \sum_{j=1}^N \mathbf{F}(\mathbf{r}_i, \mathbf{r}_j). \quad (2)$$

Thus, each cell with mobility μ attempts to maintain a self-

propelling velocity of magnitude v_0 in the direction of the unit vector $\mathbf{n}_i(t)$ and experiences intercellular forces $\mathbf{F}(\mathbf{r}_i, \mathbf{r}_j)$. The direction of the self-propelling velocity $\mathbf{n}_i(t)$, described by the angle $\theta_i^n(t)$, attempts to relax to $\mathbf{v}_i(t) = d\mathbf{r}_i(t)/dt$ with a relaxation time τ , while also experiencing angular noise ξ :

$$\frac{d\theta_i^n(t)}{dt} = \frac{1}{\tau} \arcsin\left(\left(\mathbf{n}_i(t) \times \frac{\mathbf{v}_i(t)}{|\mathbf{v}_i(t)|}\right) \cdot \mathbf{e}_z\right) + \xi, \quad (3)$$

where \mathbf{e}_z is a unit vector orthogonal to the plane of motion (see Fig. 3b) and ξ is a delta correlated Gaussian white noise term with zero mean, i.e. $\langle \xi(t) \rangle = 0$ and $\langle \xi(t)\xi(t') \rangle = \eta^2/12 \delta(t, t')$. We consider pairwise inter-cellular forces whose magnitude is a function of the distance d_{ij} between the two centers of mass only. Aiming for simplicity we present results obtained by using a piecewise linear force function, the existence of the transition we describe, however, does not depend on the specific form of the function employed. The piecewise linear force function we considered was repulsive for distances smaller than $R_{\text{eq.}}$, attractive for distances $R_{\text{eq.}} \leq d_{ij} \leq R_0$ and zero for cells farther apart, i.e.

$$\mathbf{F}(\mathbf{r}_i, \mathbf{r}_j) = \mathbf{e}_{ij} \times \begin{cases} F_{\text{rep.}} \frac{d_{ij} - R_{\text{eq.}}}{R_{\text{eq.}}} & , d_{ij} < R_{\text{eq.}} \\ F_{\text{adh.}} \frac{d_{ij} - R_{\text{eq.}}}{R_0 - R_{\text{eq.}}} & , R_{\text{eq.}} \leq d_{ij} \leq R_0 \\ 0 & , R_0 < d_{ij} \end{cases}, \quad (4)$$

where $\mathbf{e}_{ij} = \frac{\mathbf{r}_i - \mathbf{r}_j}{|\mathbf{r}_i - \mathbf{r}_j|}$, $d_{ij} = |\mathbf{r}_i - \mathbf{r}_j|$, $F_{\text{rep.}}$ is the value of the maximum repulsive force at $d_{ij} = 0$ and $F_{\text{adh.}}$ is the maximum attractive force (resulting from adhesive interactions between cells) at $d_{ij} = R_0$ (see Fig. 3b). The values $v_0 = 1$, $\mu = 1$, $\tau = 1$, $R_0 = 1$, $R_{\text{eq.}} = 5/6$, $F_{\text{adh.}} = 0.75$ and $F_{\text{rep.}} = 30$ were used, the results obtained, however, were not sensitive to the particular choice for the parameter values. The parameters of the function (4), the slope of the two linear segments ($F_{\text{rep.}}$ and $F_{\text{adh.}}$) and the equilibrium distance $R_{\text{eq.}}$, were adjusted while observing the simulations and comparing

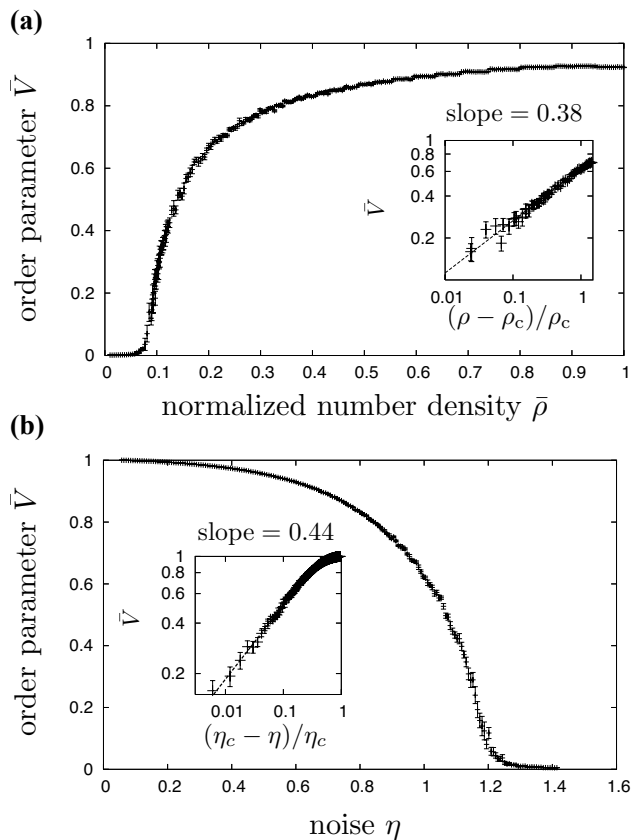


FIG. 4: The average value and standard error of \bar{V} is shown as a function of the normalized number density (a) $\bar{\rho} = \rho/\rho_{\max}$ and (b) noise η . Each data point was obtained from at least 10 independent simulation runs with $N = 1000$, with (a) $\eta = 0.6$, $\rho_{\max} \approx 2$ and (b) $\rho = 0.6$. The insets show the dependence of $\ln \bar{V}$ on (a) $(\rho - \rho_c(\eta))/\rho_c$ and (b) $(\eta_c(\rho) - \eta)/\eta_c$, the slope of the fitted lines can be associated with the critical exponents δ and β . The large scaling regimes and the similarity of the numerical values obtained for the exponents with those found for other models indicate the existence of a continuous phase transition in both ρ and η .

them with experimental videos (cf. online supplemental material), in order to achieve best possible agreement with the experiments. The two main criteria were: i.) the reproduction of the 2-dimensional sheet-like motion, wherein individual cells only interact with their nearest neighbors – i.e. cells have a well defined volume and ii) the ability of cells to “break free” from each other. The first was readily achievable by setting the slope of the repulsive force segment to be sufficiently larger than the that of the attractive segment and the value of R_{eq} , sufficiently larger than R_0 , while the second necessitated that the maximal value of the attractive segment F_{adh} , be set smaller than v_0/μ .

We carried out simulations (Fig. 3a) by solving the system of $3N$ differential equations (2) and (3) with periodic boundary conditions in systems of size $L \times L$ using a fixed time step of $\Delta t = 0.05 R_0/v_0$. The angular noise term ξ was modeled by choosing its magnitude uniformly from the interval $[-\eta/(2\sqrt{\Delta t}), \eta/(2\sqrt{\Delta t})]$. In good agreement with experi-

ments, running our model resulted in a continuous transition to the ordered phase (where all cells move in a common direction) as the number density of cells $\rho = N/(L/R_0)^2$ was increased for a fixed value of the noise $\eta = 0.6$ (Fig. 4). While varying the value of η was not experimentally feasible, simulations show that a continuous transition to the ordered phase also takes place as η is decreased while ρ is held fixed (data not shown, see online supplemental material [17]). In both cases we calculated the order parameter (1) using the velocities $\mathbf{v}_i(t_k)$ obtained from the numerical solution of (2) and (3). \bar{V} and its standard error were calculated by averaging over at least 10 independent simulation runs each at least an order of magnitude longer than the typical velocity autocorrelation time (which was found to be in the range of $10 - 1000 R_0/v_0$). The values $\rho_c = 0.18$ ($\bar{\rho}_c = 0.09$) and $\eta_c = 1.18$ were found for the critical density and noise from simulations of systems with $N = 250, 500, 1000$ and 2000 at fixed values of $\eta = 0.6$ and $\rho = 0.3$ respectively. Based on the assumption that our model exhibits a kinetic phase transition in the thermodynamic limit analogous to the continuous phase transition in equilibrium systems, we proceeded to study its critical behavior, that is,

$$\bar{V} \propto [\eta_c(\rho) - \eta]^\beta \quad \text{and} \quad \bar{V} \propto [\rho - \rho_c(\eta)]^\delta, \quad (5)$$

where β and δ are the critical exponents and $\eta_c(\rho)$ and $\rho_c(\eta)$ are the critical noise and density. Analysis of the data yielded the values $\beta = 0.44 \pm 0.08$ and $\delta = 0.38 \pm 0.07$, strongly suggesting that our model belongs to the same universality class as the angular noise model of Vicsek *et al.* [8], for which $\beta = 0.45 \pm 0.07$ and $\delta = 0.35 \pm 0.06$.

When two cells approach each other close enough, equation (3) leads to a gradual alignment of their direction of motion. Our model is in this sense similar to other models of systems of self-driven particles exhibiting emergent collective motion – i.e. flocking –, with the very important difference that the particles – the cells – do not directly use information on the movement of others around them to determine their own movement. Also, while several other models include self-propelling particles, which interact through various forces (and the seminal work of Shimoyama *et al.* [11] has alignment dynamics similar to ours), they all rely on either long-range forces [11, 14], explicit averaging [8] or both [13]. The model presented above, on the other hand, combines an experimentally motivated minimal dynamics with short-range adhesive and repulsive forces, while also displaying a continuous kinetic transition to the ordered state.

IV. EFFECTS OF BOUNDARY CONDITIONS

To investigate the effects of boundary conditions on collective cell motility, we used square as well as more complex shaped microfabricated arenas, which kept cells in a well defined area. Microstructures were fabricated by UV-curing Norland optical adhesive (NOA63) on the surface of glass cover slips using UV lithography. The typical diameter of the structures was 2 mm with 0.8 mm high walls. In closed 2D square shaped arenas we observed the roundabout motion of

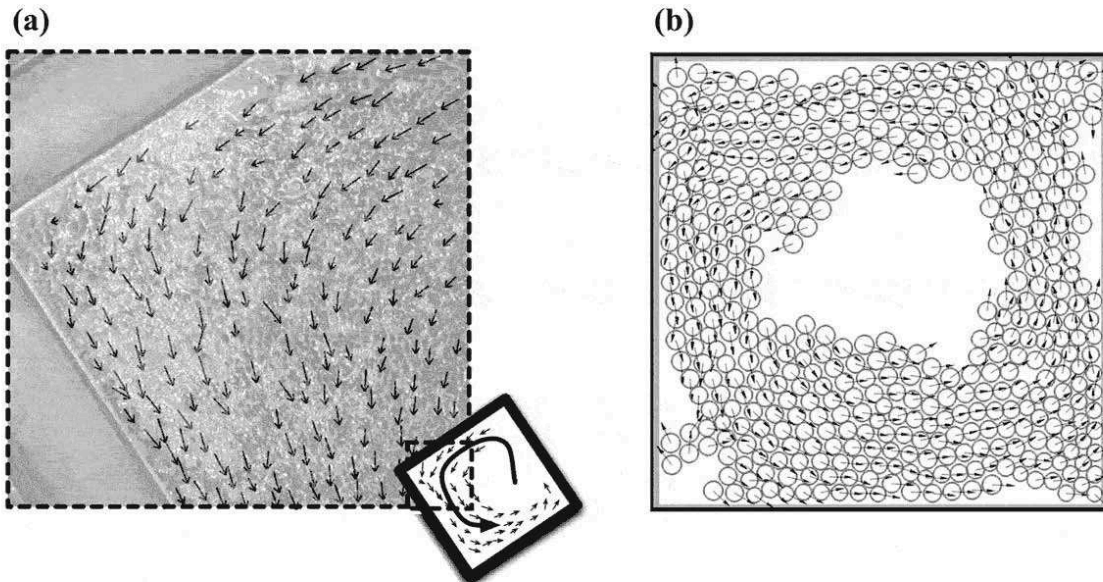


FIG. 5: (a) Experimental snapshot of a circulating cell group with the velocities of cells in the corner of a $2 \times 2 \text{ mm}^2$ square shaped microfabricated arena. (b) Simulations of model cells confined to a square arena show the emergence of circular motion over a wide range of model parameters. Supplemental video showing the circular motion of cells in the whole arena as well as in simulations are available online [17].

large cell groups. Fig. 5 shows an experimental snapshot of the circular motion with the instantaneous velocities of cells in the corner of a square shaped arena. A spectacular sustained whirling motion of the cells can be seen in the corresponding supplemental video [17].

We were also able to reproduce the above effects of boundary conditions on cell motion in simulations similar to those described in the previous section. Placing model cells in a square box with repulsive walls implemented through adding a repulsive force with an exponential falloff and finite a cutoff to the right side of equation (3) corresponding to each of the four walls

$$\mathbf{F}_w(d_{iw}) = \mathbf{n}_w \times \begin{cases} -F_{\text{wall}} \exp(-\frac{2d_{iw}}{R_0}) & , d_{iw} < R_0 \\ 0 & , R_0 < d_{iw} \end{cases} \quad (6)$$

where d_{iw} is the distance between cell $i \in \{1, N\}$ and any of the $w \in \{1, 4\}$ four walls with unit normal vector \mathbf{n}_w and $F_{\text{wall}} = 50$. In simulations cells circulated in an organized fashion under a wide range of noise and density values as well as for different system sizes. The online supplemental material [17] contains a simulation videos showing the emergence of organized circular motion of model cells confined to a square box.

V. DISCUSSION

In summary, we have presented evidence that purely short-range forces and simple experimentally motivated dynamics

can be equivalent to an effective alignment term. Drawing an analogy between our experimental and model results, we imply that the emergence of collective motion among keratocytes is an example of a continuous kinetic phase transition. Our results are also relevant in the broader context of recent work by Grégoire and Chaté [19] questioning the continuous nature of the transition in the angular noise model. Our present numerical results (exponents being similar to the ones determined for the original Vicsek *et al.* model [8]) support the view [20] that, in contrast with Ref. [19], angular noise models define a universality class with a corresponding continuous phase transition in the ordering of the velocities. We expect that our and similar experiments as well as the quantitative model of the observations we have provided for the collective motion of tissue cells will lead to a better understanding of such vital phenomena as wound healing or embryogenesis.

Acknowledgments

We are grateful to Dr. Gábor Csúcs for his instructive help in setting up a fish keratocyte lab in our institute. We thank Dr. Zsuzsanna Környei for her advice in cell culturing and Prof. Pál Ormos for the construction of the microfabricated structures. This study was supported by Hungarian Science Research Funds: NKFP 3A/0005/2002 and OTKA Nos. F49795, T049674.

-
- [1] J. K. Parrish, and W. H. Hapner (eds.) *Animal Groups in Three Dimensions* (Cambridge University Press, New York, 1997).
- [2] A. Cziráok, E. Ben-Jacob, I. Cohen and T. Vicsek: Phys. Rev. E, **54**, 1791 (1996)
- [3] W.-J. Rappel, A. Nicol, A. Sarkissian, H. Levine, and W. F. Loomis Phys. Rev. Lett. **83**, 1247 (1999)
- [4] I. H. Riedel, K. Kruse, J. Howard, Science, **309**, 300-3 (2005)
- [5] A. Jadbabaie, J. Lin, and A. S. Morse IEEE Transactions on Automatic Control, **48** 988 (2003)
- [6] H. Haga, C. Irahara, R. Kobayashi, T. Nakagaski, K. Kawabata, Biophys. J. **88**, 2250-56 (2005)
- [7] Ch. Becco, N. Vandewalle, J. Delcourt, P. Poncin, Physica A **367**, 487 (2006)
- [8] T. Vicsek, A. Cziráok, E. Ben-Jacob, I. Cohen and O. Shochet, Phys. Rev. Lett. **75**, 1226 (1995)
- [9] J. Toner and Y. Tu, Phys. Rev. Lett. **75**, 4326 (1995)
- [10] G. Grégoire, H. Chaté, and Y. Tu Physica D **181**, 157 (2003)
- [11] N. Shimoyama, K. Sugawara, T. Mizuguchi, Y. Hayakawa and M. Sano, Phys. Rev. Lett. **76**, 3870 (1996)
- [12] A. S. Mikhailov and D. H. Zanette, Phys. Rev. E **60**, 4571 (1999)
- [13] H. Levine, W.-J. Rappel and I. Cohen, Phys. Rev. E **63**, 017101 (2000)
- [14] U. Erdmann, W. Ebeling and A. S. Mikhailov, Phys. Rev. E **71**, 051904 (2005)
- [15] B. Szabó, Zs. Környei, J. Zách, D. Selmeczi, G. Csúcs, A. Cziráok and T. Vicsek, Cell Motil. Cytoskel. **59** (1), 38 -49 (2004)
- [16] T. M. Svitkina, A. B. Verkhovskiy, K. M. McQuade, G. M. Borisy, J. Cell Biol. **139** (2), 397-415 (1997)
- [17] Supplemental material including experimental and simulation videos as well as technical details of the experimental setup is available at: <http://angel.elte.hu/~bszabo/collectivecells>
- [18] D. Selmeczi, S. Mosler, P. H. Hagedorn, N. B. Larsen, H. Flyvbjerg, Biophys. J. **89** (2), 912-31 (2005)
- [19] G. Grégoire and H. Chaté Phys. Rev. Lett. **92**, 025702 (2004)
- [20] M. Nagy, I. Daruka, T. Vicsek Physica A accepted for publication